Solid State Phenomena Vol. 118 (2006) pp 125-130
Online available since 2006/Dec/15 at www.scientific.net

doi:10.4028/www.scientific.net/SSP.118.125

Low Temperature Fluidized Bed Nitriding of Austenitic Stainless Steel

E. Haruman[1,a], Y. Sun[2,b], H. Malik[1,a], A.G.E. Sutjipto[1,a], S. Mridha[1,a], K. Widi[3,c]

[1] Department of Manufacturing & Materials Engineering, Faculty of Engineering, International Islamic University Malaysia, 53100 Kuala Lumpur, Malaysia

[2]School of Materials Science and Engineering, Nanyang Technological University, Singapore 639798

[3]Department of Mechanical Engineering, ITN Malang, Indonesia, 167156

[a]esahw@iiu.edu.my; [b]asysun@ntu.edu.sg, [c]komangwidi@fti.itn.ac.id

Keywords: stainless steel, fluidized bed, nitriding, microstructure, corrosion

Abstract. In the present investigation, low temperature nitriding has been attempted on AISI 316L austenitic stainless steel by using a laboratory fluidized bed furnace. The nitriding was performed in temperature range between 400°C and 500°C. X-ray diffraction, metallography, and corrosion tests were used to characterize the resultant nitrided surface and layers. The results showed that fluidized bed process can be used to produce a precipitation-free nitrided layer characterized by the S phase or expanded austenite on austenitic stainless steel at temperatures below 500°C. But there exists a critical temperature and an incubation time for effective nitriding, below which nitriding is ineffective. The corrosion behaviour of the as-nitrided surfaces is significantly different from that previously reported for low temperature plasma nitriding. This anomaly is explained by the formation of iron oxide products and surface contamination during the fluidized process.

Introduction

Austenitic stainless steels are widely used in various sectors of industry due to their excellent corrosion resistance and fabricability. However, these materials have poor tribological properties owing to the austenitic structure and low hardness. Earlier attempts to increase the surface hardness and wear resistance of austenitic stainless steels by surface engineering, such as conventional nitriding and nitrocarburizing, led to the deterioration in corrosion resistance arising from the depletion in chromium in the hardened layer [1,2,3]. Since the mid of 1980's, attempts have been made to surface harden these materials without compromising their good corrosion resistance. These led to the development of the low temperature nitriding process [1,3-11], which is carried out at temperatures lower than 450°C. At such low processing temperatures, it was found that the nitrided layer is free from chromium nitride precipitation, and is supersaturated with nitrogen in solid solution. Such a layer is termed expanded austenite (γ_N) [5,6] or S phase [4,7,10] by some investigators. Such precipitation-free nitrided layer not only possesses high hardness and excellent wear resistance, but also possesses good corrosion resistance due to the availability of chromium in solid solution for corrosion protection.

So far, low temperature nitriding of austenitic stainless steels has been successfully conducted by various conventional and innovative techniques, including gaseous nitriding [8], plasma nitriding [3,4,5], ion beam nitriding [11] and ion implantation [9]. However, no attempts have been made by using fluidized bed process, a technique that has being increasingly used to nitride other structural steels in an industrial scale. The purpose of this work is thus to investigate the feasibility of fluidized bed nitriding austenitic stainless steels at low temperatures to form a precipitation-free layer with improved properties.

Experiment

The material used in this work is AISI 316L type austenitic stainless steel in the form of hot-rolled plate of 2 mm thickness. The plate was sectioned into nitriding coupons of 20 mm x 50 mm. Before nitriding, the specimens were cleaned by acetone.

Nitriding was carried out in a fluidized bed furnace, which uses particulate alumina as fluidized particles which flowed inside the chamber due to the flow of the nitriding gases. The specimens were heated by electrical resistance heating. Fig. 1 shows the schematic of the fluidized bed furnace. The nitriding gas composition is 25% NH_3 + 75% N_2. Prior to nitriding, the specimens were soaked in concentrated HCL solution for 15 minutes duration with the purpose to remove the native oxide film on the surface. Nitriding temperatures used are 400°C, 450°C and 500°C, for treatment times of 1 h, 3 h and 6 h respectively. After nitriding, the specimens were cooled inside the furnace down to room temperature.

The nitrided specimens were first characterised by metallographic examination and scanning electron microscopy (SEM) following standard procedures. The etchant used to reveal the microstructure is 50% HCl + 25% HNO_3 + 25% H_2O. The specimens were further characterised by surface microhardness measurements, and X-ray diffraction (XRD) analysis using Cu-Ka radiation with a vanadium filter. In addition to the analysis on the as-nitrided surfaces, X-ray depth profiling analysis was also conducted on selected specimens by successively removing layers on 4 to 6 μm thick from the surface. This facilitates the assessment of the structural variation with depth in the layer.

The electrochemical corrosion behaviour of the as-nitrided surfaces was evaluated by measuring the anodic and cathodic polarisation curves in aerated 3.0 % NaCl solution at a scan rate of 1 mV/min. The tests were conducted at room temperature by using a three electrode potentiostat with a computer data logging, requisition and analysis system. Potentials were measured with reference to the standard calomel electrode (SCE).

Results and Discussion

Metallographic examination revealed that nitriding at 400°C for times up to 6 h could not produce a continuous nitrided layer on the specimen surface. When temperature was to 450°C, nitriding was not effective for 1 h and 3 h treatments. But after 6 h nitriding, a uniform layer was formed on the surface. Fig. 2 shows the SEM micrographs of the cross sections of the specimens nitrided at 450°C for 3 h and 6 h. It can be seen that only a very thin discontinuous layer was formed after 3 h nitriding, whilst a layer about 13 μm thick was formed after nitriding for 6 h, which has a bright appearance and is resistant to the etchant used to reveal the microstructure of the substrate. As confirmed by XRD discussed later, this nitrided layer comprises mainly the S phase or expanded austenite. Below this main layer, a thin interfacial layer is evident, which is believed to be due to the accumulation of carbon in this interfacial region [12].

Increasing the temperature to 500°C resulted in the formation of a relatively thick nitrided layer after 3h and 6 h nitriding (Fig. 3). However, only a very thin layer is formed after nitriding for just 1 h (Fig. 3a). The morphology of the nitrided layers formed at this temperature for longer treatment times is different from that formed at 450°C for 6h. Some dark phases were formed in the layers (Fig. 3b and c), particularly in the upper part of the layer. The formation of such dark phases is similar to those observed for plasma nitrided samples and can be attributed to the decomposition of the S phase and the formation of chromium nitrides [7,10].

Fig. 4 shows the microhardness measured on the as-nitrided surfaces as a function of processing time for the three temperatures. It can be seen that no obvious hardening was achieved after nitriding at 400°C. The hardening effect is also insignificant after nitriding at 450°C for 1 h and 3h, and at 500°C for 1h. This corresponds well with the above metallographic examinations that no effective nitriding was achieved under these conditions.

Clearly, both structural analysis and hardness measurement indicate that under the present fluidized bed nitriding conditions, there exists an incubation time for the initiation of nitriding

reactions. Nitriding must be carried out for a duration longer than the incubation time in order to produce an effective nitrided layer. From the experimental results, it is also evident that the incubation time is temperature dependent: increasing nitriding temperature reduces the incubation time. Fig. 5 shows the plot of incubation time against nitriding temperature based on the limited experiments conducted in this work.

This incubation time phenomena, which has not been reported for other nitriding processes, such as plasma nitriding, may be related to the nature of the fluidized bed process, where the disruption of the native oxide film on the specimen surface, which is required to effect the nitriding reactions, has to rely on thermal dissociation. The higher the temperature, the faster is the dissociation of the oxide film and thus the shorter the incubation time.

Table 1 summarizes the phase compositions in the nitrided specimens as determined by XRD. The γ-austenite phase in all cases is from the substrate due to the penetration of the X-ray. Fig. 6 shows the XRD pattern from the specimen nitrided at 450°C for 6h, corresponding to the structure shown in Fig. 2b. In accordance with the findings for plasma nitriding [3-7], an S phase layer is produced with minimal chromium nitride precipitation. Increasing the nitriding temperature to 500°C resulted in the formation of CrN precipitates in the layer (Table 1). XRD depth profiling analysis (Fig. 7) revealed that more CrN nitride was formed in the upper part of the layer, corresponding to the large amount of dark phases observed in Fig. 3.b) and c). As can be seen from Fig. 7 that the relative reflection intensities from the CrN peaks decrease and those of the S phase increase with increasing distance from the surface, indicating decreasing amount of CrN precipitates.

A more detailed examination of the XRD patterns (Fig. 6 and Fig. 7) revealed the existence of iron oxide products on the as-nitrided surfaces of all specimens, even on the specimens where nitriding was not effective. The formation of oxide at the very surface could be due to the residual air in the furnace during the fluidized bed process, and this has significant effect of the corrosion behaviour of the as-nitrided surfaces, as discussed below.

Fig. 8 shows the polarisation curves measured for selected specimens. The polarisation behaviour of the untreated AISI 316L steel (Fig. 8a) is as expected, and is characterised by a well defined passive region from the corrosion potential to +40 mV (SCE). Some film breakdown occurs at this potential followed by partial reformation. At this pint the net anodic current is around 0.1 $\mu A/cm^2$. Polarisation at 180 mV leads to significant increase in current due to the occurrence of pitting corrosion. A marked difference was found for the as-nitrided surfaces, which showed much reduced corrosion resistance in terms of increased current by several orders of magnitude and the lack of passivity. Interestingly, the three as-nitrided surfaces shown in Fig. 8, which were treated at different temperatures, show very similar corrosion behaviour. Even the specimen treated at 400°C, where no effective nitrided layer was formed, exhibits poor corrosion resistance.

The observed corrosion behaviour for the fluidized bed nitrided specimens is quite different from plasma nitrided specimens reported previously [3,6,7,12], which showed good corrosion resistance in the low temperature nitrided samples. Such disagreement could be explained by the nature of the as-nitrided surface by the fluidized bed process. As mentioned above, iron oxide products were found by XRD on all the specimen surfaces, even on the 400°C treated surface. Thus, it is highly likely that the present corrosion tests only measured the corrosion of these oxide products and did not reflect the true corrosion behaviour of the nitrided cases. In order to assess the corrosion behaviour of the nitrided cases, it is necessary to remove the top superficial film on the as-nitrided surface before corrosion testing. This improved test is currently being underway and the results will be reported elsewhere.

Table 1. X-ray diffraction data of the specimens after various nitriding treatments.

Time (hrs)	400 °C	450 °C	500 °C
1	γFe,Ni (111) (200) (222)	γFe,Ni (111) (200) (222)	γFe,Ni , [S1, S2, S3 (weak)]
3	γFe,Ni (111) (200) (222)	γFe,Ni, [S1, S2, S3 (weak)]	γFe,Ni, [S1, S2, S3, (strong)] CrN
6	γFe,Ni (111) (200) (222)	γFe,Ni, [S1, S2, S3 (strong)]	γFe,Ni, [S1, S2, S3, (strong)] CrN

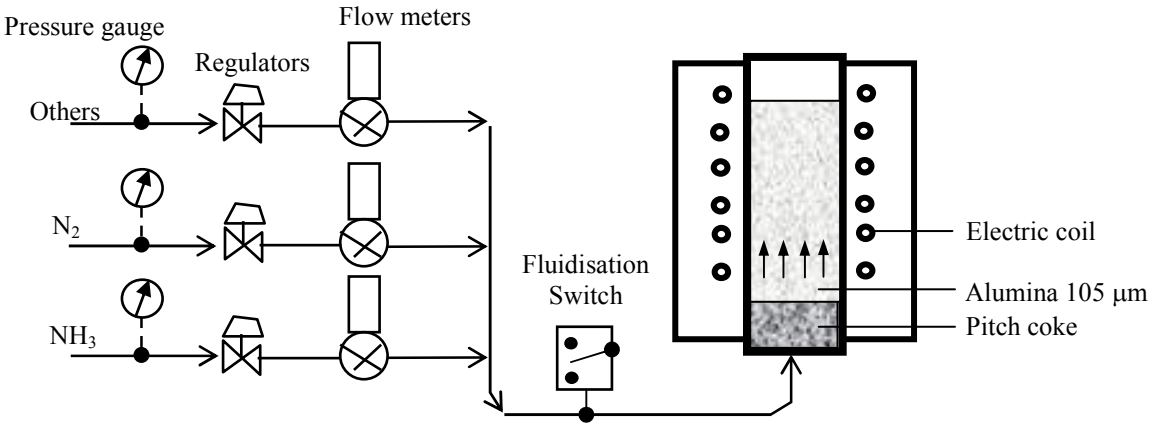

Fig. 1. Schematic picture of fluidized bed furnace.

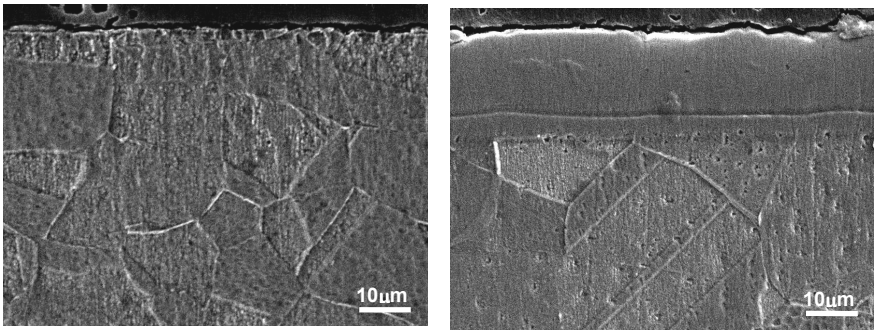

Fig. 2. SEM micrographs of 450 °C nitrided specimens: (a) 3 h, and (b) 6 h.

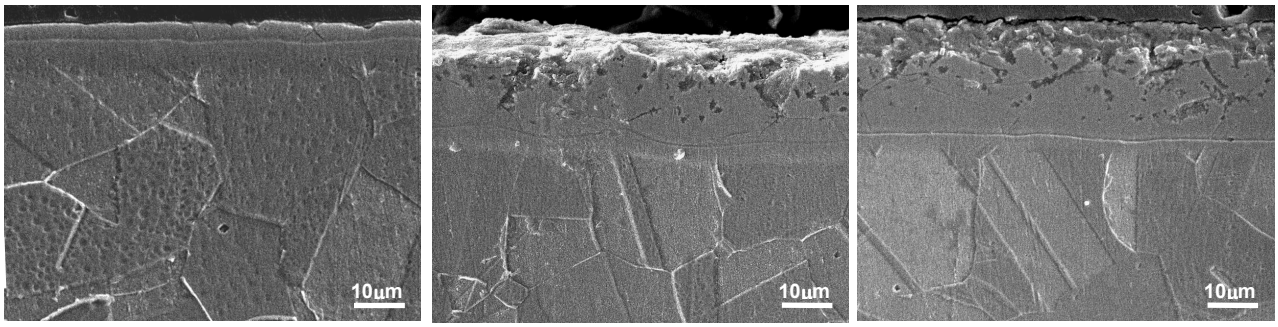

Fig. 3. SEM micrographs of 500 ºC nitrided specimens: (a) 1 h, (b) 3h, (b) and (c) 6 h.

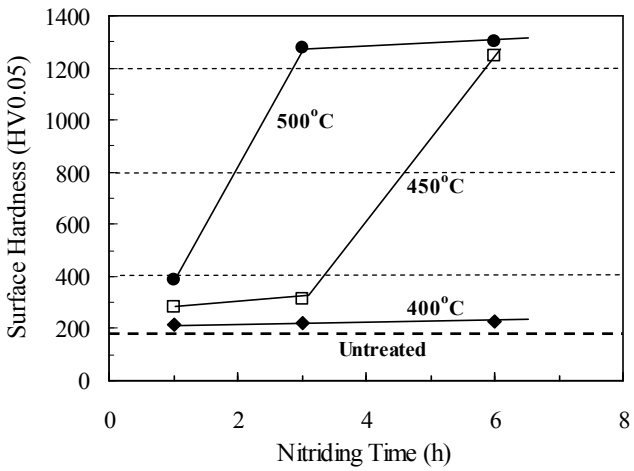

Fig. 4. Surface hardness of nitrided specimens treated under various

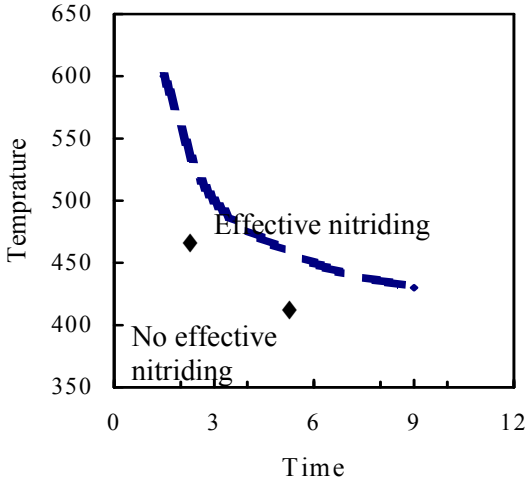

Fig. 5. Incubation time as a function of temperature.

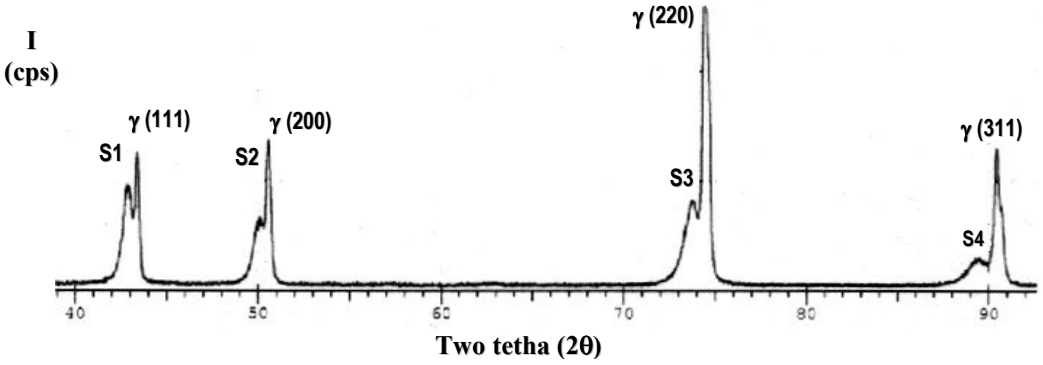

Fig. 6. XRD of nitrided specimen treated at 450 ºC for 6 hr.

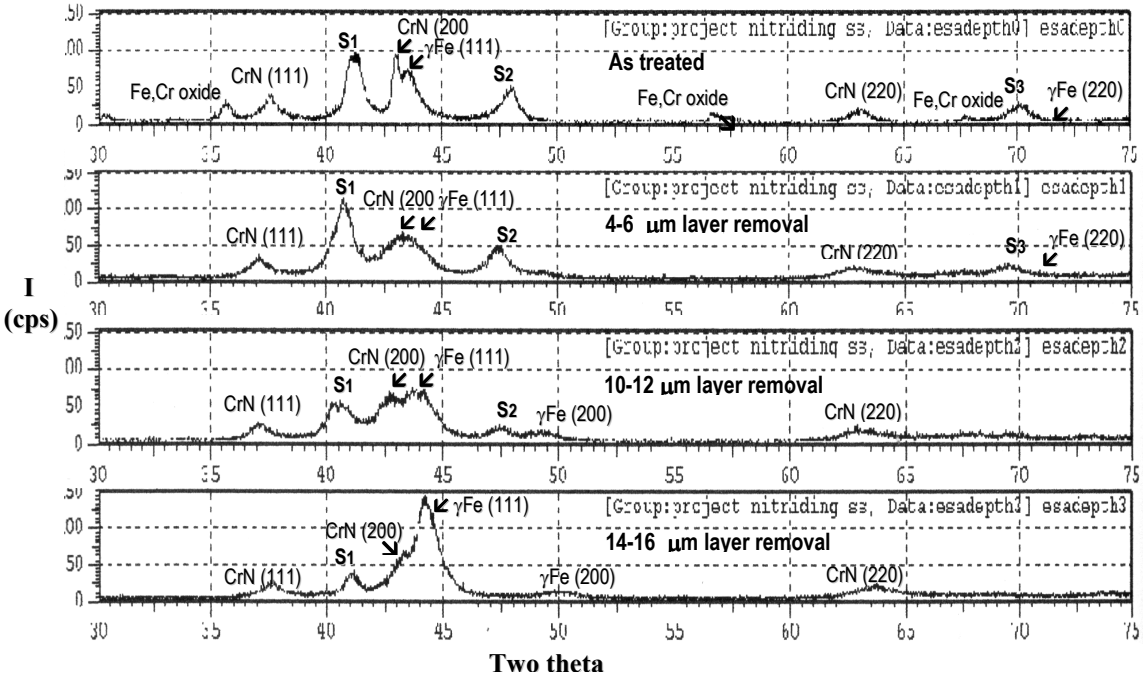

Fig. 7. XRD depth profiling of nitrided specimen treated at 500 ºC for 6 hr.

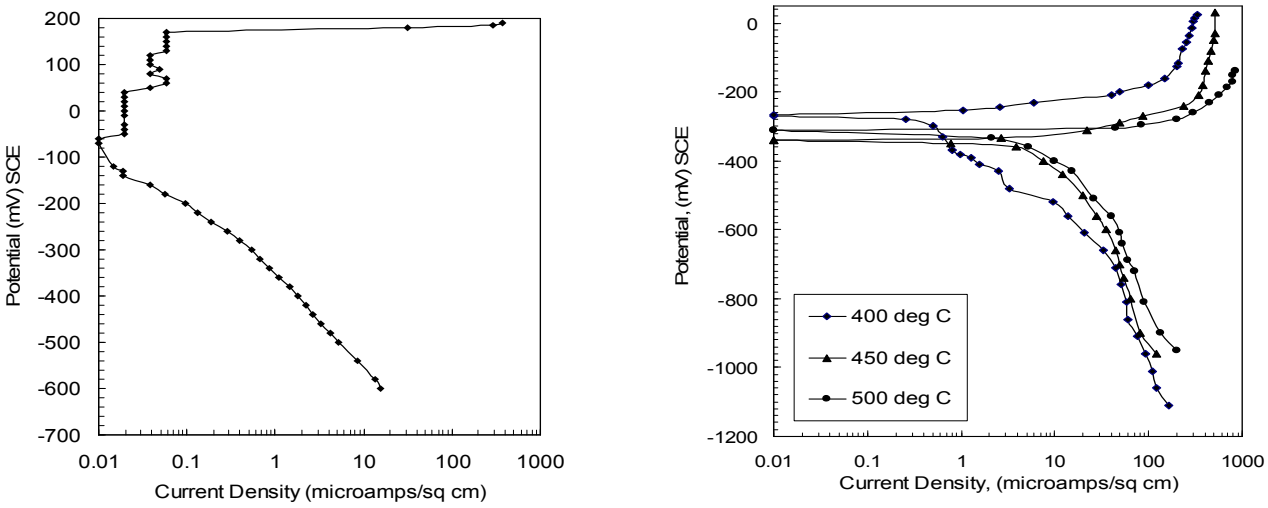

Fig. 8. Polarisation curves for (a) untreated (b) specimens nitrided for 6 h.

Conclusions

The present work on low temperature fluidized bed nitriding of AISI 316L stainless steel demonstrates that it is feasible to produce an S phase nitrided layer by the fluidized bed process. But there exists an incubation time for the initiation of effective nitriding and the incubation time decreases with increasing nitriding temperature. The structure of the nitrided layer depends on processing temperature: increasing temperature to 500°C results in the formation of a significant amount of CrN in the upper part of the nitrided layer. Corrosion testing on the as-nitrided surfaces shows disagreement with previously reported results for plasma nitrided samples. Such discrepancy can be explained by the observed formation of iron oxide products on the fluidized bed nitrided surfaces.

References

[1] T. Bell and K. Akamatsu, *Stainless steel 2000*, Maney Publ., London, 2001.

[2] E. Rolinski, Surf. Eng., Vol. 3 (1987) p. 35.

[3] Z.L. Zhang and T. Bell, Surf. Eng. Vol. 1 (1985) p. 131.

[4] K. Ichii, K. Fujimura and T. Takase, Techn. Rep. Kansai Univ. Vol. 27 (1986), p. 135.

[5] A. Leyland, D.B. Lewis, P.R. Stevenson and A. Matthews, Surf. Coat. Tech. Vol. 62 (1993) p. 608.

[6] E. Menthe, K-T. Rie, J.W. Schultze and S. Simson, Surf. Coat. Tech. Vol. 74-75 (1995) p. 412.

[7] Y. Sun, T. Bell, Z. Kolosvary and J. Flis, Heat Treatment of Metals, Vol. 26(1) (1999) p. 9.

[8] N. Yasumaru, Mater. Trans. JIM, Vol. 39 (1998) p. 1046.

[9] R. Wei, B. Shogrin, P.J. Wilbur, O. Ozturk, P.L. Williamson, I. Ivanov and E. Metin, J. Trib. Vol. 116 (1994) p. 870.

[10] Y. Sun, X.Y. Li and T. Bell, J. Mater. Sci. Vol. 34 (1999) p. 4793.

[11] L. Wang, Applied Surface Science, Vol. 211 (2003) p. 308.

[12] T. Bell and Y. Sun, Heat Treatment of Metals, Vol. 29 (3) (2002) p. 57.

[13] Y. Sun and T. Bell, Wear, Vol. 218 (1998) p. 34.

Heat Treatment of Materials
10.4028/www.scientific.net/SSP.118

Low Temperature Fluidized Bed Nitriding of Austenitic Stainless Steel
10.4028/www.scientific.net/SSP.118.125

DOI References
[6] E. Menthe, K-T. Rie, J.W. Schultze and S. Simson, Surf. Coat. Tech. Vol. 74-75 (1995) p. 12.
doi:10.1016/0257-8972(95)08246-8